

Supplement of Earth Syst. Dynam., 7, 681–696, 2016
<http://www.earth-syst-dynam.net/7/681/2016/>
doi:10.5194/esd-7-681-2016-supplement
© Author(s) 2016. CC Attribution 3.0 License.



Supplement of

Hemispherically asymmetric volcanic forcing of tropical hydroclimate during the last millennium

Christopher M. Colose et al.

Correspondence to: Christopher M. Colose (ccolose@albany.edu)

The copyright of individual parts of the supplement might differ from the CC-BY 3.0 licence.

1 **Supplemental Figure Captions**

2

3 **Figure S1.** Zonal-mean temperature anomalies as a function of atmospheric pressure and
4 latitude in CESM volcanic eruption composites for each event and season classifications
5 discussed in text.

6 **Figure S2.** GISS spatial composite of temperature anomaly ($^{\circ}\text{C}$) for (top row)
7 ASYMM_{NH}, (middle row) ASYMM_{SH}, and (bottom row) SYMM events, each in (left
8 column) NDJFM and (right column) MJJAS. Note that scaling of colorbar is different
9 from CESM composite (Figure 2).

10 **Figure S3.** As in Figure S2, except for precipitation (mm/day). Note colorbar range
11 difference compared to CESM composite (Figure 4).

12 **Figure S4.** Precipitation anomaly (mm/day) for the 1763 C.E. Laki eruption for NDJFM.
13 Results displayed for all 18 ensemble members in CESM relative to the 1757-1761 C.E.
14 NDJFM mean. Surface air temperature anomalies ($^{\circ}\text{C}$) averaged over the Niño 3.4 region
15 displayed at topright of each panel. Note colorbar range difference compared to CESM
16 all-event composite (Figure 4).

17 **Figure S5.** Precipitation asymmetry index (unitless) as defined in text vs. NH minus SH
18 AOD gradient (hemispheric sulfate loadings divided by 75 Tg for the CESM results).
19 Results displayed for both seasons in LM time series. Since most of the LM time series
20 features zero or low volcanic activity, all seasons where $-0.1 < \text{AOD gradient} < 0.1$ are
21 shown by dashed box and whisker (GISS) and solid box only (CESM). The whisker
22 lengths are very similar between the two models, and were omitted to avoid visual
23 overlap. Results presented for the 18 and 3-member ensemble mean for each season,
24 which suppresses the variability (represented by the box and whisker spread) for the non-

25 eruption compilation but allows for comparison with the ensemble-mean volcanic
26 responses.
27 **Figure S6.** Niño 3.4 SST anomalies for all ASYMM_{NH} events, centered on Year 0 (the
28 January before each eruption). The mean SST anomaly averaged over all eruption and
29 ensemble members is shown as red line, and the eruption spread is shown as gray shading
30 (after averaging 18 ensemble members). Composite-mean NH aerosol loading (Tg),
31 aligned in the same way, is shown as purple line.

32 **Figure S7.** Composite Sea Surface Height (cm) and surface wind anomalies for
33 ASYMM_{NH} events. Composite formed from the boreal winter events in Table 1 in main
34 text. Blue box shows the Niño 3.4 region.

35
36 **Figure S8.** Distribution of precipitation anomalies (mm/day) in CESM (top) and GISS-
37 E2 (bottom) during MJJAS averaged broadly over the Asian-Pacific monsoon sector
38 (65°-150°E, 10°-40°N), including regions of the Indian summer monsoon, western North
39 Pacific summer monsoon, and the East Asian summer monsoon. Each eruption is taken to
40 be an independent event, and there are more events in CESM due to the greater ensemble
41 size (note difference in y-axis scale and slightly different bin width). Solid lines
42 correspond to a normal distribution for the (red, ASYMM_{NH}; blue, ASYMM_{SH}; black,
43 SYMM) events.

44
45 **Figure S9.** Animation from May of Year -2 to December of Year +6 (as discussed in
46 text) of monthly temperature anomalies (°C) associated with ASYMM_{NH} volcanic forcing
47 in CESM. For each time step, the global aerosol loading (in Tg) and hemispheric

48 difference in loading (NH minus SH) are displayed. Months exceeding the 8 Tg global
49 aerosol loading in the G08 dataset are displayed in red.

50 **Figure S10.** As in Figure S9, except for ASYMM_{SH}.

51

52 **Figure S11.** As in Figure S9, except for precipitation (mm/day).

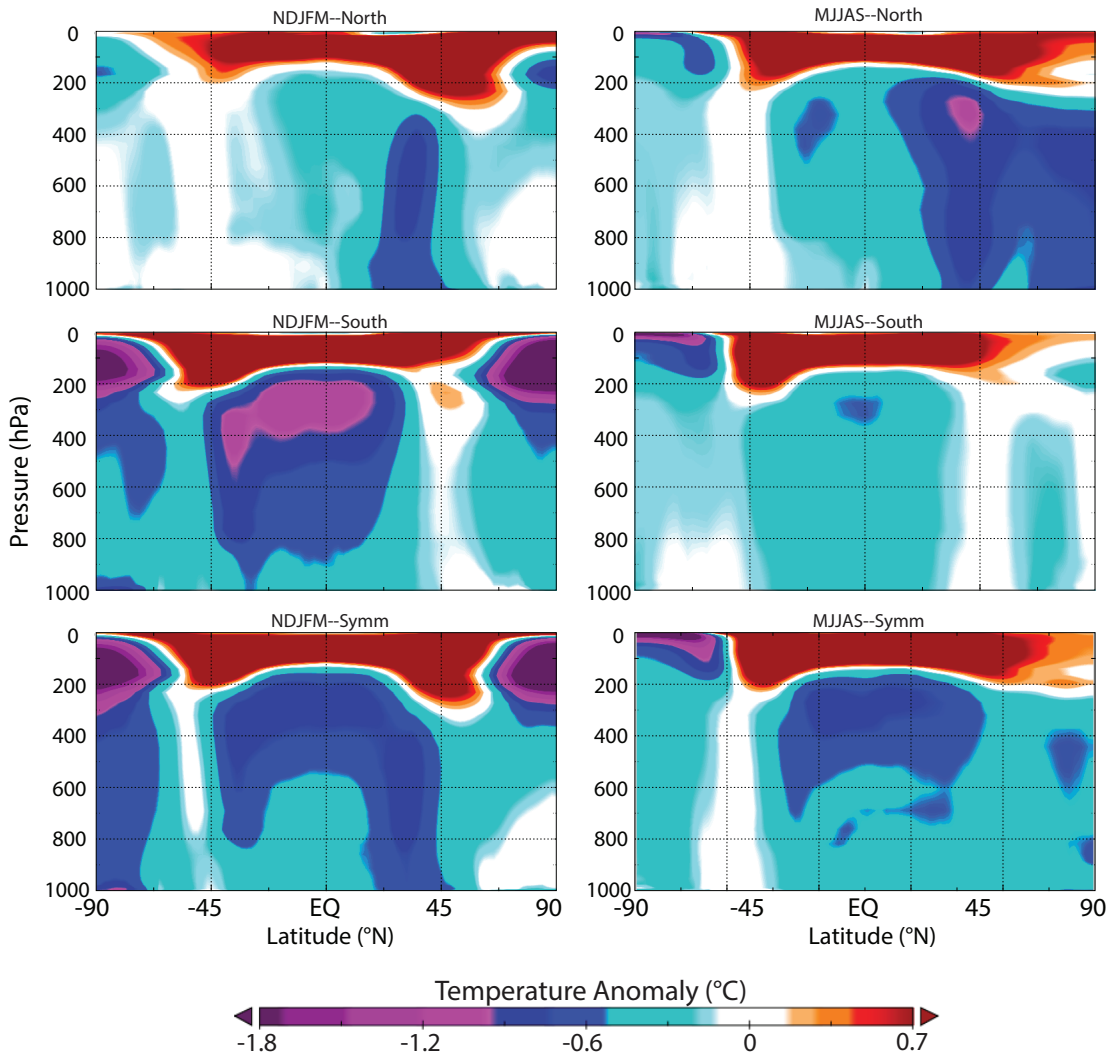
53

54 **Figure S12.** As in Figure S11, except for ASYMM_{SH}.

55

56
57
58
59
60

Temperature (Ensemble/Event Mean)

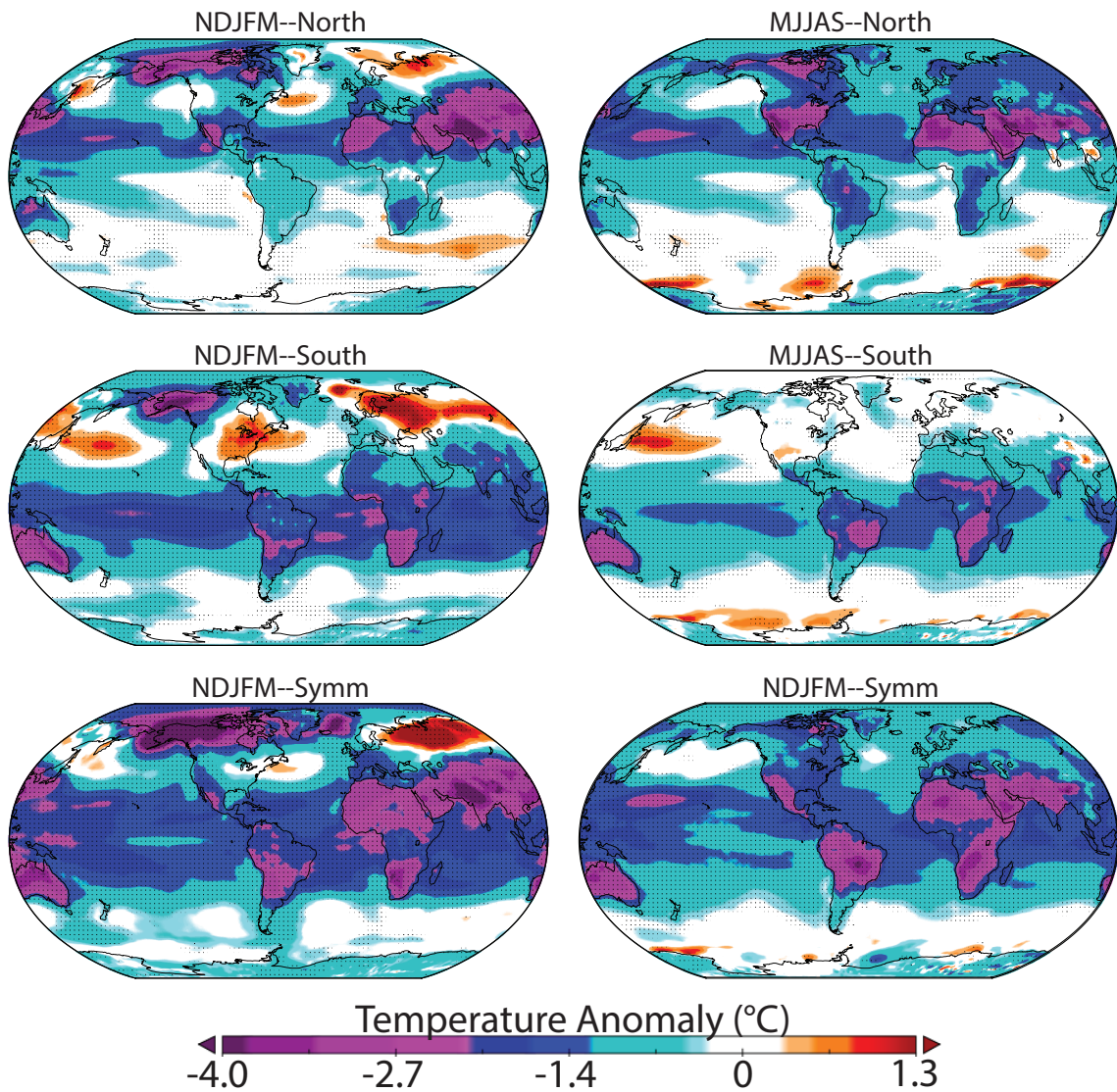


61
62
63
64
65
66

Figure S1. Zonal-mean temperature anomalies as a function of atmospheric pressure and latitude in CESM volcanic eruption composites for each event and season classifications discussed in text.

67
68
69
70
71
72
73
74
75
76

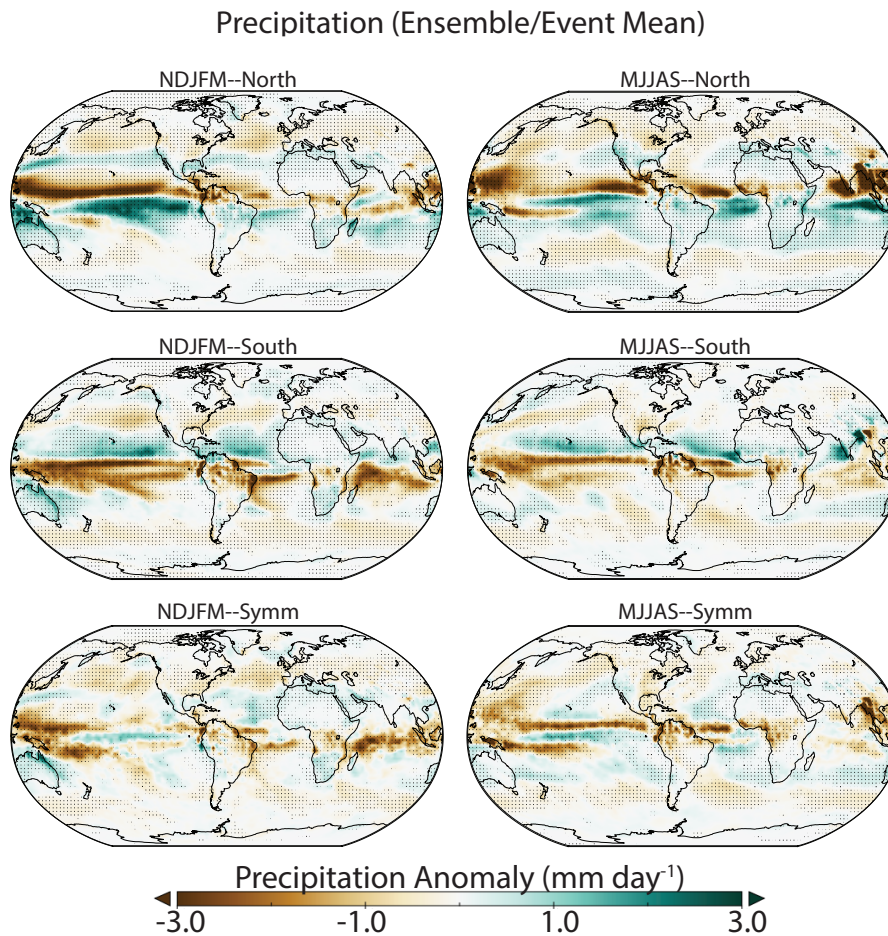
Temperature (GISS Ensemble/Event Mean)



77
78

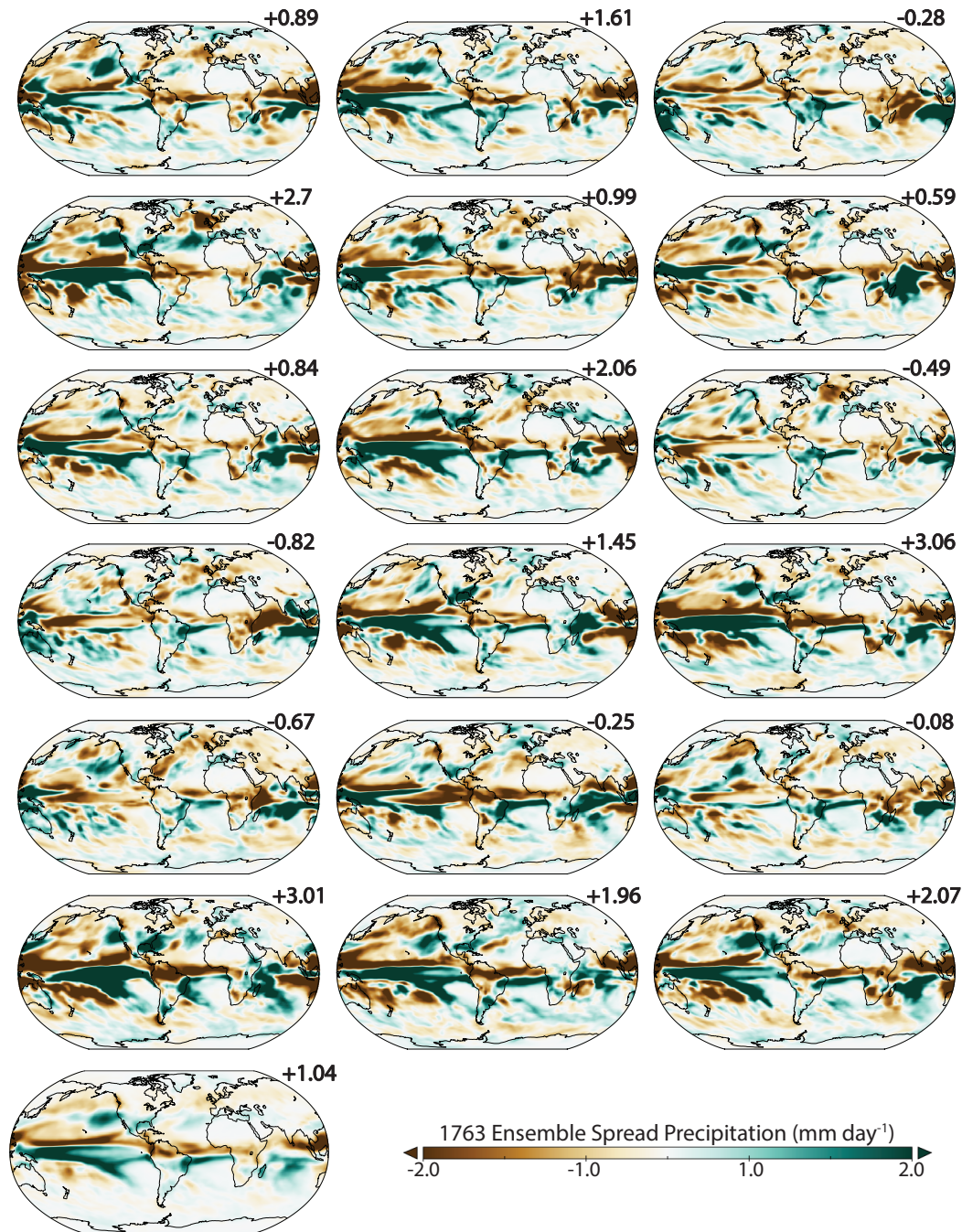
Figure S2. GISS spatial composite of temperature anomaly ($^{\circ}\text{C}$) for (top row)

79 ASYMM_{NH}, (middle row) ASYMM_{SH}, and (bottom row) SYMM events, each in (left
80 column) NDJFM and (right column) MJJAS. Note that scaling of colorbar is different
81 from CESM composite (Figure 2).

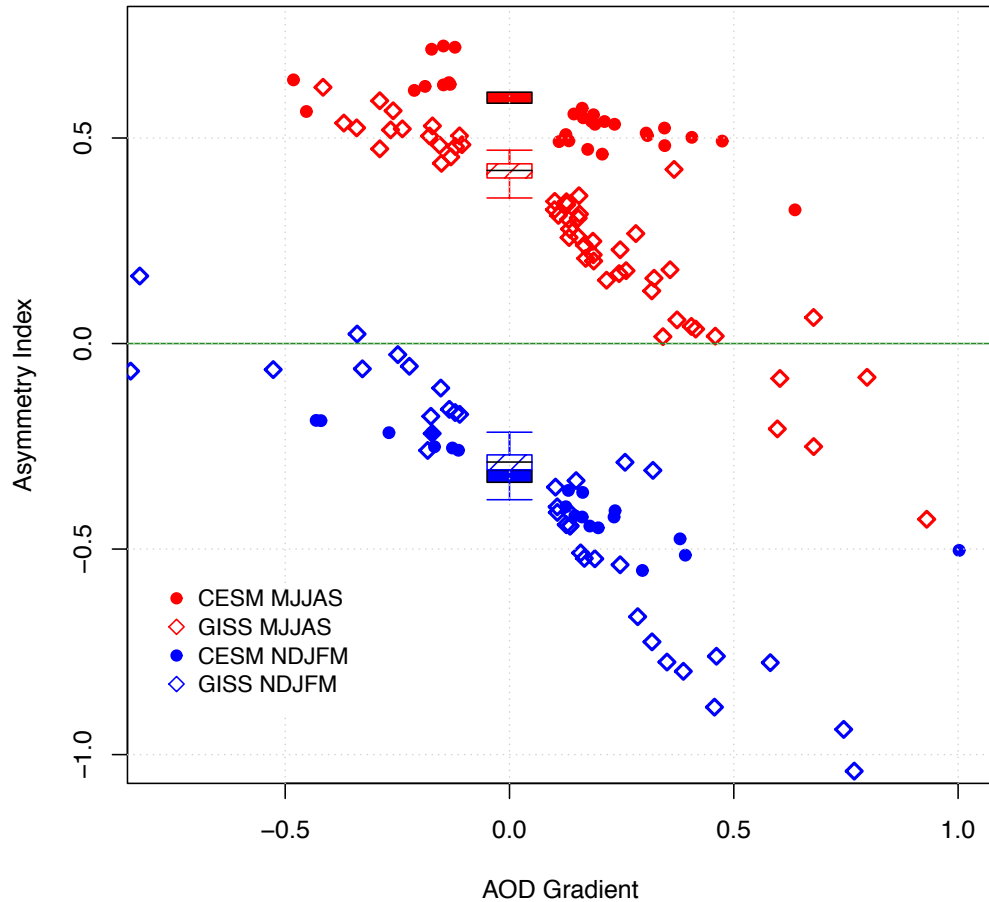


82
83 **Figure S3.** As in Figure S2, except for precipitation (mm/day). Note colorbar range
84 difference compared to CESM composite (Figure 4).

85



86
 87 **Figure S4.** Precipitation anomaly (mm/day) for the 1763 C.E. Laki eruption for NDJFM.
 88 Results displayed for all 18 ensemble members in CESM relative to the 1757-1761 C.E.
 89 NDJFM mean. Surface air temperature anomalies ($^{\circ}\text{C}$) averaged over the Niño 3.4 region
 90 displayed at topright of each panel. Note colorbar range difference compared to CESM
 91 all-event composite (Figure 4).



92
 93 **Figure S5.** Precipitation asymmetry index (unitless) as defined in text vs. NH minus SH
 94 AOD gradient (hemispheric sulfate loadings divided by 75 Tg for the CESM results).
 95 Results displayed for both seasons in LM time series. Since most of the LM time series
 96 features zero or low volcanic activity, all seasons where $-0.1 < \text{AOD gradient} < 0.1$ are
 97 shown by dashed box and whisker (GISS) and solid box only (CESM). The whisker
 98 lengths are very similar between the two models, and were omitted to avoid visual
 99 overlap. Results presented for the 18 and 3-member ensemble mean for each season,
 100 which suppresses the variability (represented by the box and whisker spread) for the non-
 101 eruption compilation but allows for comparison with the ensemble-mean volcanic
 102 responses.

103 CESH LME uses the Parallel Ocean Program (POP2; Smith et al. 2010) as the
104 ocean model component. This is where the sea surface temperature (SST) and sea surface
105 height (SSH) diagnostics presented in Figure S6 and S7 are calculated. The model
106 features 384 (latitude) x 320 (longitude) ocean grid points, with variable horizontal
107 resolution that increases toward the tropics. There are 60 vertical levels, gradually
108 increasing from 10 m resolution in the top 150 m to ~250 m below 3 km depth.

109 To perform a superposed epoch analysis for the state of the Pacific following all
110 ASYMM_{NH} events, the Niño 3.4 index is calculated for each ensemble member in CESH
111 (averaging the SST from 120°W-170°W, 5°S-5°N) with the long-term annual cycle
112 removed. “Year 0” corresponds to the January before each eruption. We only show
113 results for ASYMM_{NH}, since no distinguishable behavior in the Niño 3.4 time series is
114 exhibited for the other eruption classifications, as discussed in text. Months before Year 0
115 may feature a non-zero aerosol loading (as in Figure S6) due to the 8 Tg threshold for
116 defining an eruption not being satisfied, or due to overlap with previous eruptions. Unlike
117 the spatial composites discussed in the main text, pre-eruption months presented below
118 are not replaced with the pre-eruption dates of previous overlapping eruptions. However,
119 in the composite-mean, the aerosol loading is negligible for pre-eruption years, as well as
120 after ~5 years after the composite eruption, and does not bias the results.

121 Figure S6 presents the Niño 3.4 time series averaged over all ASYMM_{NH}
122 eruptions and ensemble members. Grey shading corresponds to the eruption spread after
123 averaging over the ensemble members. Since the CESH ENSO amplitude is large, even
124 after averaging over 18 members, the pre-eruption envelope is still quite wide (individual

125 events may be on the order of 5°C above normal). Averaging over fewer ensemble
126 members would progressively increase the width of the envelope.

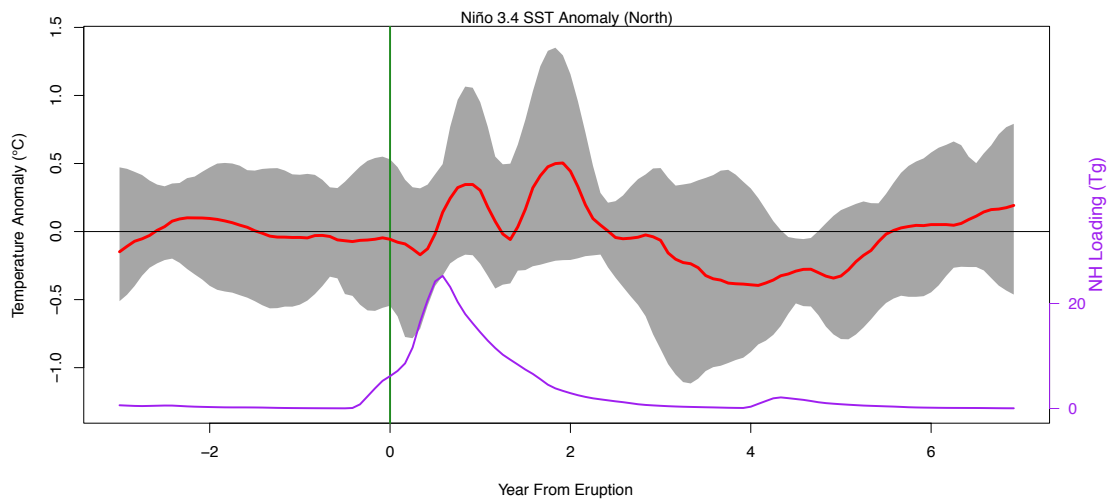
127

128

129

130

131



132

133 **Figure S6.** Niño 3.4 SST anomalies for all ASYMM_{NH} events, centered on Year 0 (the

134 January before each eruption). The mean SST anomaly averaged over all eruption and

135 ensemble members is shown as red line, and the eruption spread is shown as gray shading

136 (after averaging 18 ensemble members). Composite-mean NH aerosol loading (Tg),

137 aligned in the same way, is shown as purple line.

138

139

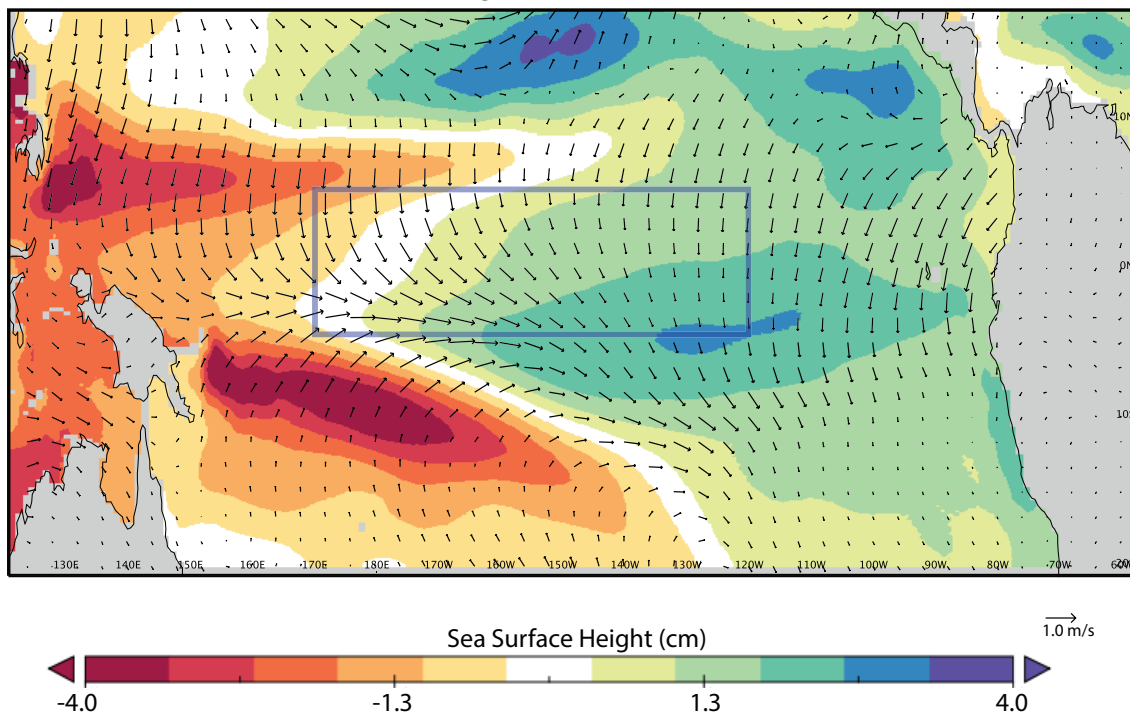
140

141

142

143

Sea Surface Height and Surface Wind Anomalies (North)



144

145

Figure S7. Composite Sea Surface Height (cm) and surface wind anomalies for

146

ASYMM_{NH} events. Composite formed from the boreal winter events in Table 1 in main

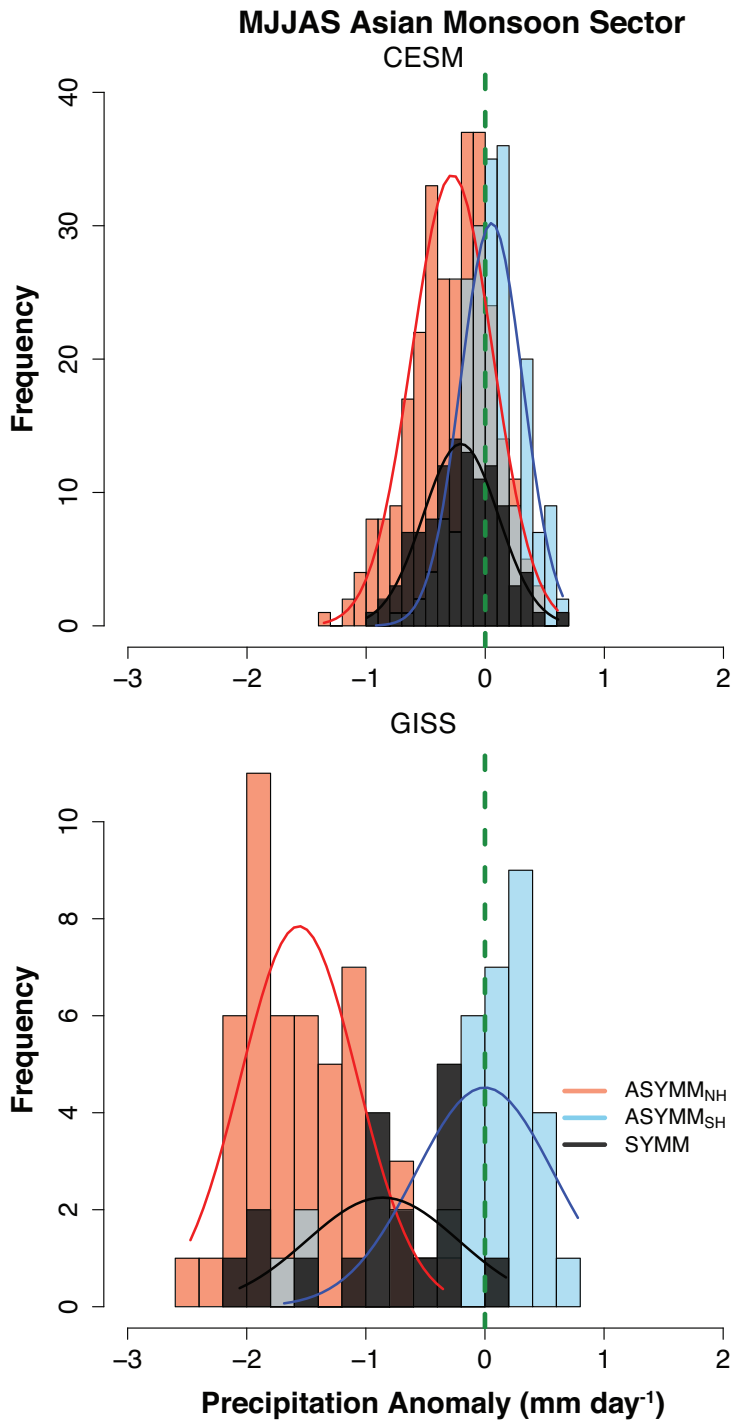
147

text. Blue box shows the Niño 3.4 region.

148

149

150



151
 152 Figure S8. Distribution of precipitation anomalies (mm/day) in CESM (top) and GISS-E2
 153 (bottom) during MJJAS averaged broadly over the Asian-Pacific monsoon sector (65°-
 154 150°E, 10°-40°N), including regions of the Indian summer monsoon, western North
 155 Pacific summer monsoon, and the East Asian summer monsoon. Each eruption is taken to
 156 be an independent event, and there are more events in CESM due to the greater ensemble
 157 size (note difference in y-axis scale and slightly different bin width). Solid lines
 158 correspond to a normal distribution for the (red, ASYMM_{NH}; blue, ASYMM_{SH}; black,
 159 SYMM) events.

161 In the animations below, monthly temperature and precipitation anomalies from
162 CESM (for each event, using five years as a pre-eruption reference period) are shown in a
163 loop from May of Year -2 to December of Year +6, where year 0 and month 1
164 corresponds to the January before each eruption, defined based on the same criteria as in
165 main text. The animation shows the average anomaly field for all eruptions among 18
166 ensemble members, which suppresses the internal variability in pre-eruption months.
167 There is still variability in the sequence of pre-eruption composites due to the finite
168 number of realizations of natural variability, non-zero aerosol loading (only when the 8
169 Tg global aerosol loading is exceeded is an event aligned with Year 0), overlap with
170 previous eruptions, in addition to non-volcanic radiative forcings that are still present in
171 13/18 of the ensemble members.

172

173 <https://av.tib.eu/media/18569?48>

174

175 **Figure S9.** Animation from May of Year -2 to December of Year +6 (as discussed in
176 text) of monthly temperature anomalies ($^{\circ}\text{C}$) associated with ASYMM_{NH} volcanic forcing
177 in CESM. For each time step, the global aerosol loading (in Tg) and hemispheric
178 difference in loading (NH minus SH) are displayed. Months exceeding the 8 Tg global
179 aerosol loading in the G08 dataset are displayed in red.

180

181 <https://av.tib.eu/media/18571?16>

182 **Figure S10.** As in Figure S9, except for ASYMM_{SH} .

183

184 <https://av.tib.eu/media/18570?32>

185 **Figure S11.** As in Figure S9, except for precipitation (mm/day).

186

187 <https://av.tib.eu/media/18572?0>

188 **Figure S12.** As in Figure S11, except for ASYMM_{SH} .

189

190

191

192

193 **References**

194 Smith, R. D., et al.: The Parallel Ocean Program (POP) reference manual, Ocean component of

195 the Community Climate System Model (CCSM), Tech. Rep. LAUR-10-01853, 141 pp., Los

196 Alamos Natl. Lab., Los Alamos, N. M., 2010.